Human Identification Using KnuckleCodes

Ajay Kumar, Yingbo Zhou
Department of Computing
The Hong Kong Polytechnic University
Hung Hom, Kowloon, Hong Kong
Email: ajaykr@ieee.org, 08509610g@polyu.edu.hk

***Abstract*—The usage of finger knuckle images for personal identification has shown promising results and generated lot of interest in biometrics. In this work, we investigate a new approach for efficient and effective personal identification using *KnuckleCodes*. The enhanced knuckle images are employed to generate *KnuckleCodes* using localized Radon transform that can efficiently characterize random curved lines and creases. The similarity between two *KnuckleCodes* is computed from the minimum matching distance that can account for the variations resulting from translation and positioning of fingers. The feasibility of the proposed approach is investigated on the finger knuckle database from 158 subjects. The experimental results, *i.e.*, equal error rate of 1.08% and rank one recognition rate of 98.6%, suggest the utility of the proposed approach for online human identification.**

I. Introduction

Research efforts for human identification using peg-free hand imaging have shown high interest in the biometrics literature. Palmprint [1], hand geometry [2], palm vein [3], palm dorsal vein patterns [4] have been investigated as an alternative (or compliment) to the more popular fingerprint identification. However, the research efforts to investigate the utility of finger knuckle patterns for personal identification have been very limited. As a result, there is no known use of knuckle pattern identification in commercial or civilian applications.

The anatomy of human hands is quite complicated and intricate but highly responsible for the individuality of hand-based biometrics. The finger skin surface is highly rich in texture which consists of palmer friction ridges and palmer flexion creases [5]. The palmside hand surface regions are highly popular for personal identification and employed to acquire fingerprint, palmprint and hand shape features. The back surface of hands is plainer as it has no specialized functions. While fingers bend forward and assist in grasping the objects against palm, its backward motion is resisted.

There are *tendons* running along the back of the fingers that assist in extending the fingers when required. However, if fingers are attempted to be bent past certain points, the tendons will hyper-extend, injuring the fingers. The unidirectional bending of fingers generates highly unique pattern formations, on the finger surface joining proximal phalanx and the middle phalanx bones, and employed for the finger knuckle based identification.

A. Related Work

The human identification using 3D and 2D finger surface details have generated lot of research interest and promising results have been detailed in the literature [6]-[10]. Woodard and Flynn [6] have demonstrated that finger knuckle surface is quite distinctive 3D surface and detailed the user identification from range images using curvature and shape-based index. The usage of range images to extract distinctive 3D finger geometrical features is also detailed in [2], [7]. Recently, reference [8] has detailed the usage of finger knuckle surface for online user identification using combination of sub-space features. This paper also describes the simultaneous extraction and usage of geometrical features for performance improvement. The image details from the palmside finger surface can also be employed for the user identification as detailed in [9] and [10]. However, the texture details/patterns that can be acquired from low-resolution palmside finger surface imaging are very limited but useful in improving the performance from the simultaneously acquired palm surface (palmprint) as detailed in [9]-[10].

B. Selecting a Finger

Our approach in the selection of one of the fingers for the human identification is motivated by the anatomical studies [11]. The forefinger and little finger have very high mobility and agility. The ring finger is regarded as the clumsiest and stiffest of all fingers. Therefore the ring

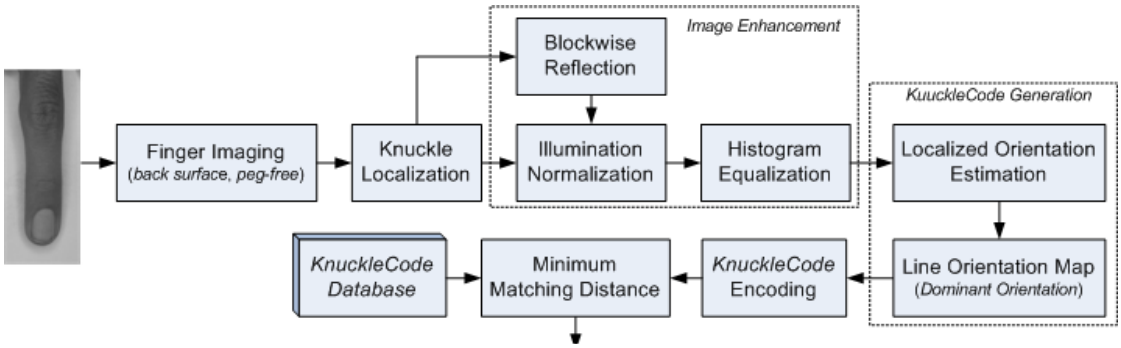

Figure 1: Block diagram for the human identification using finger knuckles.

[†] finger offered high user inconvenience even with the peg-free imaging considered in this work. The middle finger offered higher surface area and higher stability in acquiring knuckle patterns. Therefore middle fingers images were selected for evaluating knuckle identification. It may also be noted that the comparative evaluation of performance from the four finger knuckle images in [8] suggested that middle finger achieves the best performance. It is also possible to acquire four fingers simultaneously, as in [8], and improve the performance from the combination since four knuckle patterns present quite distinct texture.

II. Block Diagram

The block diagram for the proposed personal identification system using finger knuckles is shown in figure 1. The backside (knuckle side) fingers images are conveniently acquired from a digital camera for the identification. Each of these images requires localization of region of interest for the feature extraction. This region of interest is the region having maximum knuckle creases and automatically extracted using the edge detection based approach detailed in reference [8]. The extracted knuckle images have non uniform illuminations and therefore require image enhancement. The enhanced knuckle images are employed for the feature extraction. The feature extraction approach employed in this work is detailed in section III and generates binarized codes *KnuckleCodes* for each of the localized pixel positions. The extracted knuckles are used to match with those in the database stored during the user registration. The extracted knuckle images have wide translational and rotational variations which have to be accounted during matching stages. Therefore the matching distance employed in this work is based on comparison in the neighborhood and is detailed in section IV. The user identity is ascertained from the identity associated with the *KnuckleCodes* that generates minimum matching distance.

III. Knuckle Image Enhancement

The finger surface is highly curved and results in uneven reflection which also generates shadow. The knuckle images therefore have low contrast and uneven illuminations. These undesirable effects are reduced in the pre-processing step using nonlinear image enhancement. The image enhancement steps employed in this work are summarized as follows:

(a) Each of the knuckle images is divided into 10×10 pixels sub-blocks, and the gray-level in each of the blocks is computed by summing up all pixel values in this block and then divided by a constant N. Selecting N = 256 achieved the desirable enhancement performance in our experiments. The gray-level in each block represents the average background illumination from the corresponding sub-block.

(b) The estimated *blockwise* average from (a) is used to construct a background illumination image, of the same size as original knuckle image, using bi-cubic interpolation.

(c) The background illumination image from (b) is subtracted from the original image for the normalization of uneven illumination. The resulting normalized image is subjected to the histogram equalization to obtain the final enhanced knuckle image.

Figure 2 shows a sample of finger knuckle image and the corresponding steps to obtain the enhanced image. It can be noticed from figure 2(d) that the employed steps for the image enhancement have been quite successful in improving the illumination and the contrast of the finger knuckle images.

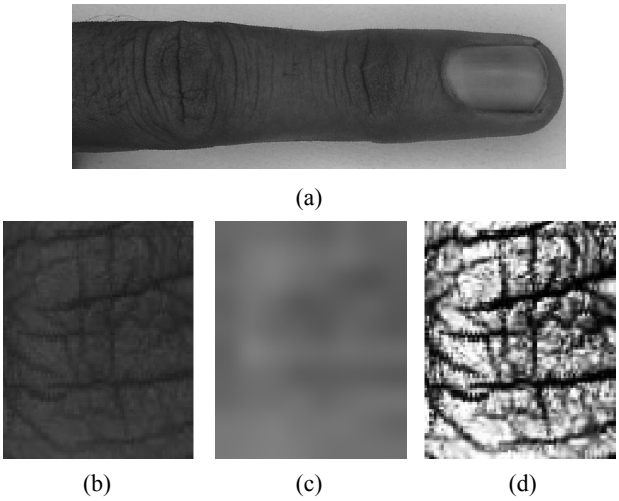

(a)

(b) (c) (d)

Figure 2: (a) Finger image, (b) segmented finger knuckle image, (c) mean bi-cubic image, (d) enhanced knuckle image.

IV. Feature Extraction

The enhanced knuckle image mainly consists of curved lines and creases. Therefore the feature extraction approaches that are highly successful in the characterization of such random textured biometric traits (*e.g*., iris, palm, *etc*.) deserve investigation. There were two key factors in the selection of feature extraction approach for our system. Firstly, the localized estimation of features, rather than the global estimation, was preferred as such approaches have shown to deliver better performance. Secondly, the computational complexity another factor as the developed system is intended for the online user identification.

The feature extraction approach is focused on the detection and characterization of curved knuckle lines and creases from the enhanced finger knuckle images. The Radon transform can effectively accentuate such line features by summation of image pixels along several directions and is highly computationally efficient. However the lines and creases in the images are curved rather than linear along image dimensions, therefore localized Radon transform was employed for the feature extraction.

A. Localized Radon Transform

The localized Radon transform (LRT) for a discrete image $g[m\ ,n]$ on a finite grid R_q^2 can be defined as:

[†] The ring finger is also known as *toe finger* since it has no more mobility than a toe.

$$s[X_p] = \mathrm{M}_i(p) = \sum_{(x,y)\in X_p} g[x,y] \quad (1)$$

where $R_q = \{0, 1, \ldots, q-1\}$, q is a positive integer, and R_q^2 is centred at (x_0, y_0). The X_p represents set of points on R_q^2 such that

$$X_p = \{(x,y): y = p(x - x_0) + y_0, x \in R_q\} \quad (2)$$

where p denotes the slope of X_p, *i.e.* slope of line passing through the centre (x_0, y_0) of R_q^2. The LRT is not an invertible transform but useful to represent line and crease like features. The line width of X_p can be empirically selected corresponding to the width of the observed knuckle lines in the acquired finger images. In this work, this line width is therefore empirically selected as two pixels. Figure 3 shows the computation of LRT for the width of X_p equals 2, when the localized region of 14×14 pixels ($l = 14$) is selected in 6 ($D = 6$) directions. The main objective of employing LRT in our approach is to *efficiently* and *effectively* ascertain the orientation p of knuckle lines and creases in a localized region.

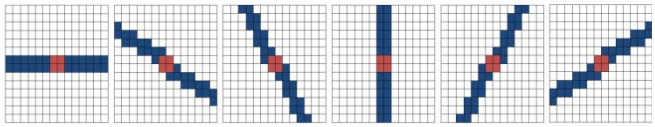

Figure 3: Computing localized Radon transform in a 14×14 pixel region in the directions of $0°, \pi/6, \pi/3, \pi/2, 2\pi/3, 5\pi/6$ and the X_p is 2 pixels wide.

B. KnuckleCodes Using LRT

The orientation of curved lines and creases is estimated from the localized magnitude of LRT. This orientation for every pixel centred at (x_0, y_0) on R_q^2 is estimated from the summation of pixels along the line of given slope p. It should be noted that the curved knuckle lines (figure 2) appear as dark lines, *i.e.*, identified from the pixel gray-levels which are smaller than the background. Therefore minimum, rather than maximum, magnitude of $s[X_p]$ is of interest. The index of the dominant direction at every pixel forms the feature and is computed as follows:

$$\theta_p(x_0, y_0) = \arg(min_p(s[\mathrm{X}_p])), \; p = 1, 2, \ldots, D \quad (3)$$

where the $\theta_p(x_0, y_0)$ represents the line direction or the dominant index of pixel $g[x_0, y_0]$. This operation is repeated as the centre of lattice R_q^2 moves over all the pixels in the image. The dominant direction θ_p at every pixel is binary coded using Z binary bits and is referred to as *KnuckleCode* in this paper. The binarized encoding of orientation index from every pixel is preferred mainly for the efficient template storage and matching. In order to effectively handle the pixels localized at the edges of images, zero padding is employed for such boundary pixels. As long as the padding pixel values are same, the dominant direction $\theta_p(x_0, y_0)$ will not be influenced by such padding. This guarantees the correctness of the algorithm in computing $\theta_p(x_0, y_0)$ for boundary pixels.

V. Matching KnuckleCodes

The matching of two *KnuckleCodes*, extracted from two different fingers, should be robust to handle the translation and rotational variations in the localized knuckle images. These variations can be either due the translation and/or rotation of presented fingers (due to peg-free imaging) and/or due to the inaccuracies in the localization of knuckle image regions. These inaccuracies can also be due to the influence of the shadows resulting from the highly curved 3D finger surface. Therefore, the approach employed in this work attempts to generate the best possible matching score while considering the translation and rotation of fingers that sometimes present partially matching knuckles.

The matching score between two Z bit *KnuckleCodes* **R** and **T**, obtained from two corresponding knuckle images, is generated as follows:

$$S(\mathbf{R}, \mathbf{T}) = \min_{\forall i\in[0,2\mathrm{w}], \forall\, j\in[0,2\mathrm{h}]} \left(\sum_{x=1}^{\mathrm{m}} \sum_{y=1}^{\mathrm{n}} \phi \left(\widehat{\mathbf{R}}(x+i, y+ \right. \right. \\ \left. \left. j, \mathbf{T}x, y \right. \right. \quad (4)$$

where $\widehat{\mathbf{R}}$ represents the *KnuckleCodes* (acquired during user registration) with the width and height expanded to $\mathrm{m} + 2\mathrm{w}$ and $\mathrm{n} + 2\mathrm{h}$, while

$$\mathrm{w} = \mathrm{floor}\left(\frac{\mathrm{m}}{3}\right), \; \mathrm{h} = \mathrm{floor}\left(\frac{\mathrm{n}}{3}\right), \quad (5)$$

$$\widehat{\mathbf{R}}(\mathrm{x}, \mathrm{y}) = \begin{cases} \mathbf{R}(x-w, y-h) & x \in [w+1, w+\mathrm{m}], \; y \in [h+1, h+\mathrm{n}] \\ -1 & \text{otherwise} \end{cases}, \quad (6)$$

$$\phi(J_b, K_b) = \begin{cases} 0 & if \;\; J_b = K_b \; \forall \, b \\ 1 & otherwise \end{cases} \quad (7)$$

where b = 1, 2, ..Z which denotes binary bits for the Z bit *KnuckleCodes* while m and n denotes the width and height of *KnuckleCodes*, *i.e.*, size of **R** and **T**. It may be noted that the size of *KnuckleCodes* is significantly smaller than the original knuckle image size and depends on the local region size X_p (one fourth of the knuckle image size for $X_p = 2$) employed in this work. The *KnuckleCodes* can be considered similar to *FingerCodes* [13] or *IrisCodes* [14] as they also represent the localized texture information.

VI. Experiments

The proposed approach for human identification using knuckle images is rigorously evaluated on finger image database from 158 subjects. This database was acquired over a period of 11 months and each subject/volunteer contributed five image samples which resulted in total of 790 images. These images were acquired using a digital camera in an indoor environment using unconstrained (peg-free) setup as detailed in [8]. The middle finger images from each of the subjects are employed to automatically extract 80×100 pixel knuckle region using the segmentation method detailed in [8]. Figure 2(a) shows a sample of acquired middle finger image and correspondingly segmented knuckle image in figure 2(b). The segmented images have low contrast and may suffer from

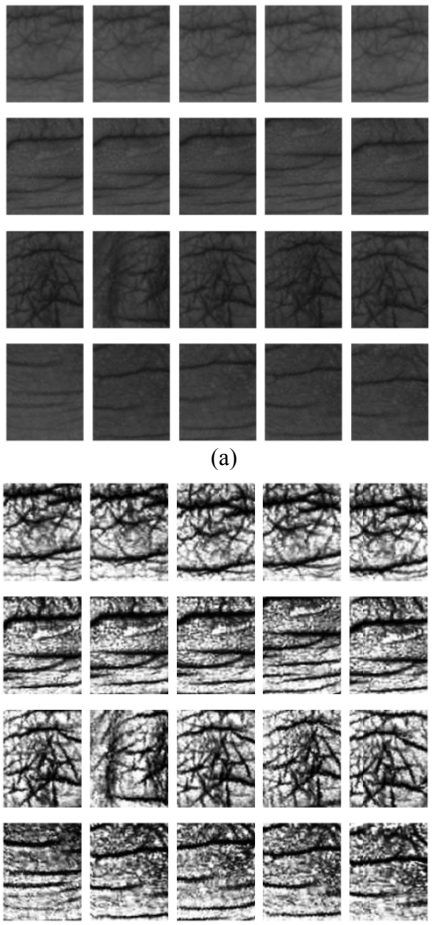

Figure 4: Finger knuckle image samples from the five users ii (a), and the corresponding enhanced image samples in (b)

non-uniform illumination. Therefore each of the knuckle images were enhanced as detailed in section II. The five knuckle image samples from the four subjects are shown in figure 4(a) and the corresponding enhanced image samples are reproduced in figure 4(b).

The enhanced knuckle images are subjected to the feature extraction using LRT as detailed in section III. The total number of candidate directions (D) for every pixel is empirically fixed to 8. The performance evaluation is achieved by 5-fold cross validation and the average of experimental results is presented. This represents a more realistic experiments, similar to as in [9], as the knuckle images have large variations within the same class resulting from shadows, illumination and pose changes. The gray level representation of *KnuckleCodes* generated from the Knuckle image sample in figure 5(a) is shown in figure 5(b)-(c). The

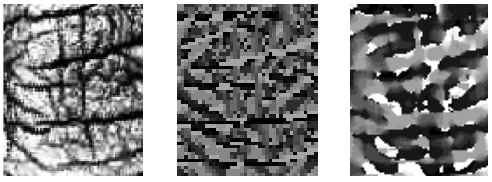

Figure 5: Gray level representation of *KnuckleCodes* generated for knuckle image in (a) using LRT in (b), and using even Gabor filters in (c).

receiver operating characteristics (ROC) using 790 (158×5) genuine and imposter 124030 ($158 \times 157 \times 5$) matching scores is shown in figure 6. The comparison of experimental results from our approach, with the appearance based approach, *i.e.*, *eigenknuckles* and *fisherknuckles* employed in [8] on the database employed in this work is also shown in figure 6. Table 1 summarizes the best case average equal error rate from the experiments. We also performed experiments for the recognition and the corresponding comparative cumulative match characteristics (CMC) are shown in figure 7.

Another possible approach for extracting orientation features is to employ real part of Gabor functions and ascertain the orientation at every pixel using the maximum filtered response. Such an approach has been investigated on the palmprint data in [15] and achieves promising results. Therefore the generation of *KnuckleCode* using such Gabor filters is also investigated and the comparative results are shown in figure 6-7. The twelve real Gabor filters, with 15×15 mask size, centred at frequency of $1/(2\sqrt{2})$ were employed to achieve the best performance. Smaller or larger number of filters and mask sizes generated poor performance. The experimental results in figure 6 and figure 7 suggests that the performance from the *KnuckleCodes* generated using LRT, *i.e., KnuckleCodes* (Radon), is far superior as compared to those from real Gabor filter based encoding.

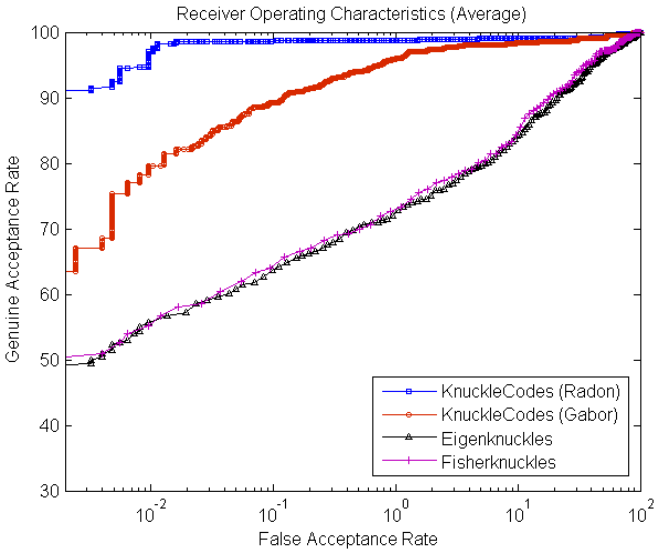

Figure 6: The ROC curves from the experiments.

Table 1: Comparative performance from the experiments.

	Equal Error Rate			
EER (%)	*KnuckleCodes* (Radon)	*KnuckleCodes* (Gabor)	*EigenKnuckles*	*Fisherknuckles*
Mean	1.08	2.66	13.92%	12.66%
Std deviation	1.08	1.81	1.24	1.27%

Table 2: Performance analysis using Localized Radon Transform.

	Equal Error Rate					
X_p	1		2	3		4
l	13	15	14	13	15	14
Mean (%)	1.15	1.15	**1.08**	2.78	2.53	6.96
Std deviation (%)	1.57	1.57	1.08	0.96	1.48	0.9

The experimental results from the LRT using 8 directions (D = 8) for various parameters, *i.e.* X_p (figure 3, equation 2) and l (summation length, figure 3), are illustrated in table 2. In order to clearly define the centre of the LRT parity of line width (width of X_p) and length (l) must be the same, *i.e.* both are even or odd, so while the line width is equal to 1 and 3 line length 13 and 15 are used. Table 3 illustrates the comparative experimental results from the *KnuckleCodes* generated using LRT and even Gabor filters. The number of even Gabor filters at every pixel defines the extraction of possible orientation information (directions D) that can be acquired for *every pixel* in the knuckle image. The experimental results in table 3 suggests that the best results are achieved when the total number of even Gabor filters are fixed to 12. However, little better results are obtained when the total number of directions are fixed to 8 (as compared to 12), for the case when *KnuckleCodes* are generated using LRT.

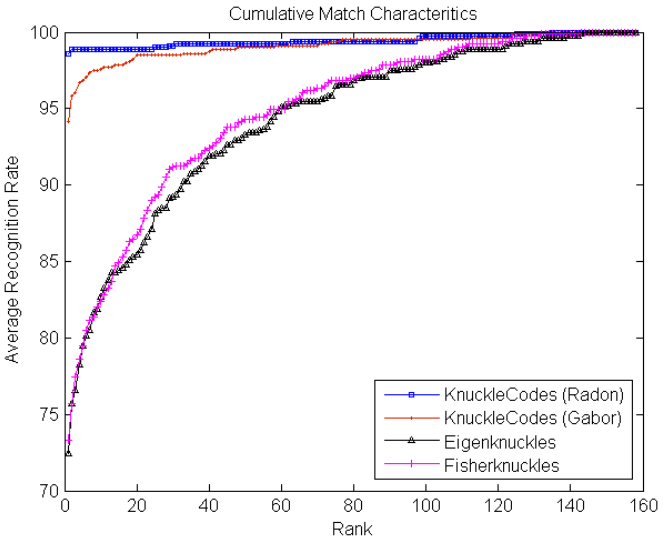

Figure 7: The CMC curves from the experiments.

Table 3: Comparative performance analysis with the variations in D.

		Equal Error Rate					
D (Intervals in 0-π)		6	8	10	12	14	16
KnuckleCodes (Radon)	Mean (%)	2.03	**1.08**	1.29	1.14	1.27	1.29
	Std deviation (%)	1.37	1.08	1.59	1.37	1.60	1.24
KnuckleCodes (Gabor)	Mean (%)	4.18	11.14	5.82	**2.66**	3.29	7.59
	Std deviation (%)	2.31	1.88	1.04	1.81	2.26	2.24

A. Discussion

It may also be noted that the generation of *KnuckleCodes* using Gabor filters is highly computationally demanding as it requires convolution operation at every pixel and orientation as compared to simple sum in LRT. Therefore, the *KnuckleCodes* generated from LRT are also favourably suitable for online user identification. It should be noted that reference [8] simultaneously employs hand geometry features while reference [9] [10] employed palmside finger/palm features. Therefore any direct comparison of our results, that employed only middle finger knuckle images, with [8]-[10] is difficult. The accuracy of segmenting knuckle images from the presented fingers highly influences the matching scores between the corresponding *KnuckleCodes*. In order to handle the rotational and translational variations in the segmented knuckle images, we employed minimum of matching score (4) generated from the translation of respective templates in the region that extended to one third of length and width of the templates. The finger knuckle image database employed in this work is being made available [17] to encourage further research efforts in knuckle biometrics.

VII. Conclusion

This paper has investigated a new approach for human identification using finger knuckle images. The orientation of curved finger knuckle lines and creases are extracted as template, referred to as *KnuckleCodes*, and employed for the human identification. The *KnuckleCodes* extractied using LRT achieves the best results as compared to various approaches investigated in this paper. The advantage of using Radon transform based *KnuckleCodes*, lies not only in significantly higher performance, but also in the template storage and matching (the size/dimension of *KnuckleCodes* is one fourth of the corresponding dimension of knuckle image or 25 × 20). In summary, the experimental results from the finger knuckle identification approach investigated in this paper achieves significantly promising results, *i.e.*, average rank-one recognition rate of 98.6% and equal error rate of 1.08% on the database of 158 persons. These results can be attributed to extraction of reliable *orientation features* using LRT, usage of robust knuckle image enhancement technique, and importantly to the generation of reliable matching distances using equation (4)-(7) that can also account for the translation of finger knuckles.

The orientation of palm-lines and creases has been exploited for the personal identification using Gabor functions [15] and Radon transform based features [12]. However, the finger knuckles present more attractive

alternative than palmprints, mainly because of its smaller surface area, think/rich lines and creases, and importantly due to large possibility of higher user acceptance. The user acceptance for employing finger knuckle in human identification is expected to be very high as there is no stigma of personal information (fortune telling beliefs, *i.e*. life-line, heart-line, head-line, *etc*.) associated with finger knuckle lines/creases.

This paper has offered promising and computationally smaller alternative for the finger knuckle identification. However, much more needs to be done and investigated as there exits lot of potential from finger knuckles for the human identification. There have not been any studies to ascertain the stability of finger knuckles with age, time, varying medical and environmental conditions. Further work is also required to ascertain the individuality of finger knuckles in large population (say more than 1000 subjects) and on the dermatoglyphics analysis to ascertain the variation of knuckle patterns across the population.

REFERENCES

[1] A. Kumar, "Incorporating cohort information for reliable palmprint authentication," *Proc. ICVGIP*, Bhubaneswar, India, pp. 583–590, Dec. 2008.

[2] V. Kanhangad, A. Kumar, D. Zhang, "Combining 2D and 3D hand geometry features for biometric Verification," *Proc. CVPR'09 Biometrics Workshop*, Miami, Florida, Jun. 2009.

[3] J.-G. Wang, W.-Y. Yau, A. Suwandy, and E. Sung, "Person recognition by fusing palmprint and palm vein images based on "Lapacianpalm" representation," *Pattern Recognition*, vol. 41, pp. 1531–1544, 2008.

[4] L. Wang, G. Leedham and Siu-Yeung Cho, "Minutiae Feature Analysis for Infrared Hand Vein Pattern Biometrics," *Pattern Recognition*, 41 (3), pp. 920-929, 2008.

[5] A. K. Jain and M. Demirkus, "On latent palmprint matching, MSU Technical Report, May 2008

[6] D. L. Woodard and P. J. Flynn, "Finger surface as a biometric identifier", *Computer Vision and Image Understanding*, vol. 100, no. 3, pp. 357-384, Dec. 2005.

[7] S. Malassiotis, N. Aifanti, and M. G. Strintzis, "Personal authentication using 3-D finger geometry," *IEEE Trans. Inf. Forensics Security*, vol. 1, no. 1, pp. 12–21, Mar. 2006.

[8] A. Kumar and Ch. Ravikanth, "Personal authentication using finger knuckle surface", *IEEE Trans. Info. Forensics & Security*, vol. 4, no. 1, pp. 98-110, Mar. 2009

[9] S. Ribaric, and I. Fratric, "A Biometric identification system based on eigenpalm and eigenfinger Features", *IEEE Trans. Pattern Anal. Mach. Intell.*, vol. 27, no. 11, Nov. 2005.

[10] Y. Hao, T. Tan, Z. Sun and Y. Han, "Identity verification using handprint," *Proc. ICB 2007*, Lecture Notes Springer, vol. 4642, pp. 328-337, 2007.

[11] R. W. Young, "Evolution of the human hand: the role of throwing and clubbing," *J. Anat*., 202(1), pp. 165-174, Jan. 2003.

[12] W. Jia, D.-S. Huang, and D. Zhang, "Palmprint verification based on robust line orientation code," *Pattern Recognitio*n, vol. 41, pp. 1504-1513, 2008.

[13] A.K. Jain, S. Prabhakar, L. Hong, and S. Pankanti, "FingerCode: A filterbank for fingerprint representation and matching," *Proc. CVPR*, vol. 2, pp. 187-193, 1999.

[14] J. Daugman, "Probing the uniqueness and randomness of IrisCodes: Results from 200 billion iris pair comparisons," *Proc. IEEE,* vol. 94, no. 11, pp 1927-1935, 2006.

[15] A. W. K. Kong and D. Zhang, "Competitive coding scheme for palmprint verification", *Proc. 17th ICPR*, Washington, DC, pp. 1051-4651, 2004.

[16] V. Onana, E. Trouvé, G. Mauris, J.-P. Rudant, and E. Tonyé, "Detection of linear features in synthetic-aperture radar images by use of localized radon transform," *Applied Optics*, vol. 43, no. 2. Jan. 2004.

[17] http://web.iitd.ac.in/~biometrics/knuckle/iitd_knuckle.htm